Journal of Alloys and Compounds 643 (2015) S159–S164

Contents lists available at ScienceDirect

Journal of Alloys and Compounds

journal homepage: www.elsevier.com/locate/jalcom

Efficient KF loaded on MgCaAl hydrotalcite-like compounds in the transesterification of *Jatropha curcas* oil

Ariel Guzmán-Vargas [a,*], Teresa Santos-Gutiérrez [a], Enrique Lima [b], Jorge L. Flores-Moreno [c], Miguel A. Oliver-Tolentino [a], María de J. Martínez-Ortiz [a]

[a] ESIQIE-IPN, Departamento de Ingeniería Química, Laboratorio de Investigación en Materiales Porosos, Catálisis Ambiental y Química Fina, UPALM Edif.7 P.B. Zacatenco, México D.F. 07738, Mexico
[b] IIM-Universidad Nacional Autónoma de México, Circuito exterior s/n, Cd. Universitaria, 04510 México DF, Mexico
[c] UAM-Azcapotzalco, Área de Química de Materiales, Av. San Pablo 180, Col. Reynosa Tamaulipas, 02200 México DF, Mexico

ARTICLE INFO

Article history:
Available online 17 January 2015

Keywords:
LDH
Hydrotalcite
Mixed oxides
Physicochemical characterization
Transesterification
Biodiesel

ABSTRACT

In this work a series of MgCaAl hydrotalcite-like compounds were synthetized by coprecipitation method at constant pH. In order to obtain the catalysts, the samples were modified with KF by incipient wetness impregnation at different wt%, after that, they were dried and calcined to obtain the mixed oxides. The effect of divalent cations ratio and KF load were studied in the transesterification reaction of *Jatropha curcas* oil to obtain biodiesel employing an inedible oil. XRD analysis showed typical diffraction patterns of LDH, by nitrogen physisorption the LDH mesoporous structure was also confirmed, ^{27}Al NMR spectra showed bands at 10 and 88 ppm attributed to the Al coordination before and after thermal treatment. While for the impregnated samples after calcination the profiles exhibited the mixed oxide formation, in addition, another peaks appeared associated to the formation of various fluorinated species as shown by XRD, additionally, ^{19}F NMR showed a main signal at −180 ppm indicating the presence of active tetrahedral aluminum fluoride species.

The reaction evolution was monitoring calculating the oil conversion to biodiesel by integration of the signal spectra using ^{1}H NMR spectroscopy. The results of catalytic tests in transesterification reaction showed a direct correlation between Mg/Ca ratio and KF content in the oil conversion to biodiesel, the higher conversion was achieved (90%) when Mg/Ca = 1 and KF load was 30 wt%.

1. Introduction

Most of biodiesel is today produced via homogeneous catalysis by the triglycerides transesterification reaction of refined/edible type oils using methanol and an alkaline catalyst. The crude glycerol and biodiesel obtained, which are separated by settling after catalyst neutralization, are then purified involving such as in a huge amount of wastewater, product-separation problems, and limits of raw materials. Heterogeneous catalytic process, employing solids materials with diverse nature such as solid base, acid, and immobilized enzymes, have been studied as alternative to replace the homogeneous catalyst [1].

In this context, a wide variety of nanostructured solid catalysts have been reported showing good catalytic activity for biodiesel production using different oils: modified zeolites as Na-X, Na-Y, Cs-Y [2], zirconia supported as WO_3/ZrO_2, TiO_2/ZrO_2, Al_2O_3/ZrO_2 [3–5], supported alumina modified with different alkali salts: KI, KF, KNO_3, K_2CO_3, and KOH, recently the system $K_2CO_3/Al_2O_3–SiO_2$ was reported [6–10], mixed oxides or oxides: MgO, CaO–MgO, $CuO–Al_2O_3$, $CoO–Al_2O_3$, $MnO–Al_2O_3$, and various mixed oxides resulting from hydrotalcite-like compounds [11–19], heteropoly-acids [20–22] among others solid materials, these studies point out the effect of the base–acid properties in the reaction of transesterification.

In particular, modified Layered Double Hydroxides (LDHs) or hydrotalcite-like compounds prove to be a promising alternative due to their acid–base properties, especially when these materials are calcined to obtain the corresponding mixed oxides. Structurally, the LDHs are formed from the arrangement of brucite ($Mg(OH)_2$) structure giving gibbsite type sheets or layers. A fraction substitution of divalent cation, Mg^{2+}, for trivalent cations produce a positive charge layer which is compensated by negativily charged species, e.g. anions intercalated between the sheets. Hydrotalcite-like compounds can be represented by the general formula $[M^{2+}_{1-x}M^{3+}_{x}(OH)_2]^{x+}$ $(A^{n-})_{x/n}\cdot mH_2O$, where M^{2+} (M = Mg, Ca,

* Corresponding author.
E-mail address: aguzmanv@ipn.mx (A. Guzmán-Vargas).

http://dx.doi.org/10.1016/j.jallcom.2015.01.029
0925-8388/

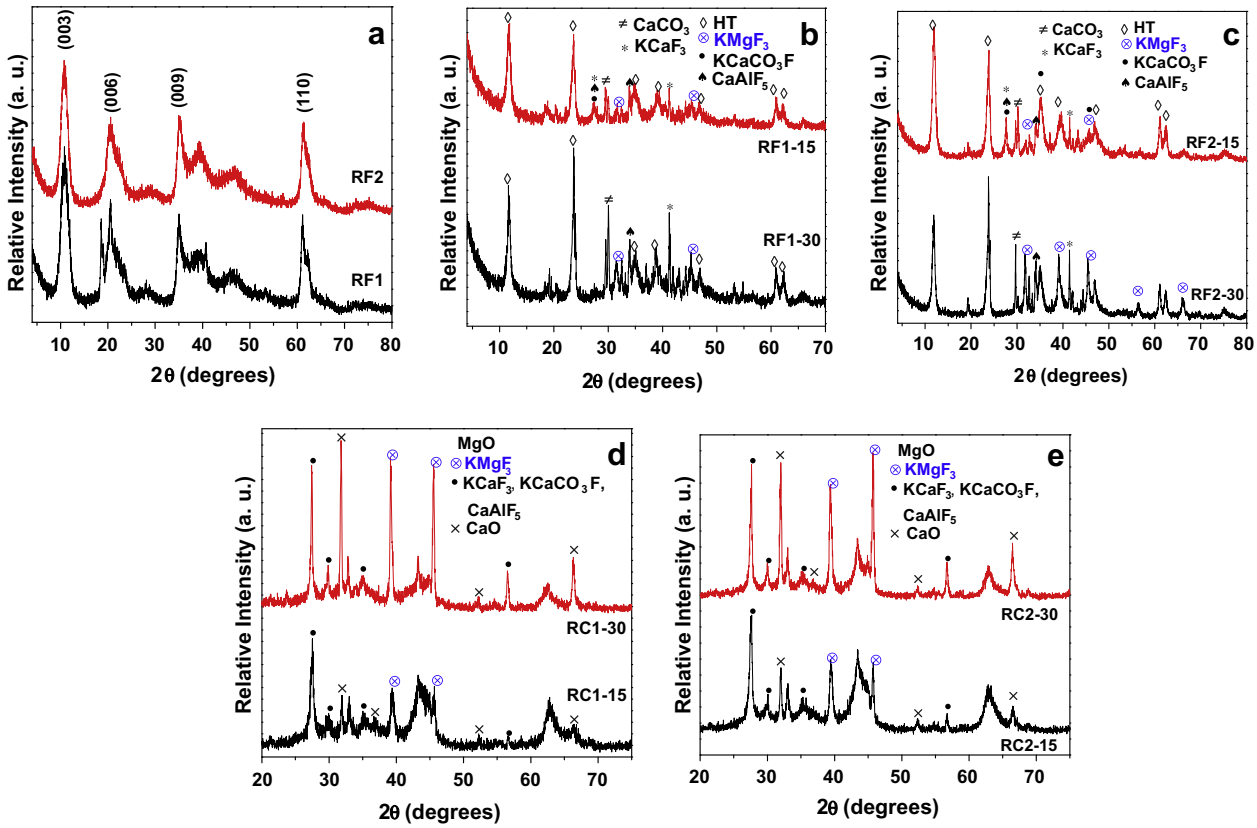

Fig. 1. XRD patterns for (a) the as-synthetized MgCaAl LDH, (b) fresh KF-loaded MgCaAl LDH (Mg/Ca = 1), (c) fresh KF-loaded MgCaAl LDH (Mg/Ca = 2), (d) calcined KF/MgCaAl LDH (Mg/Ca = 1), and (e) calcined KF/MgCaAl LDH (Mg/Ca = 2).

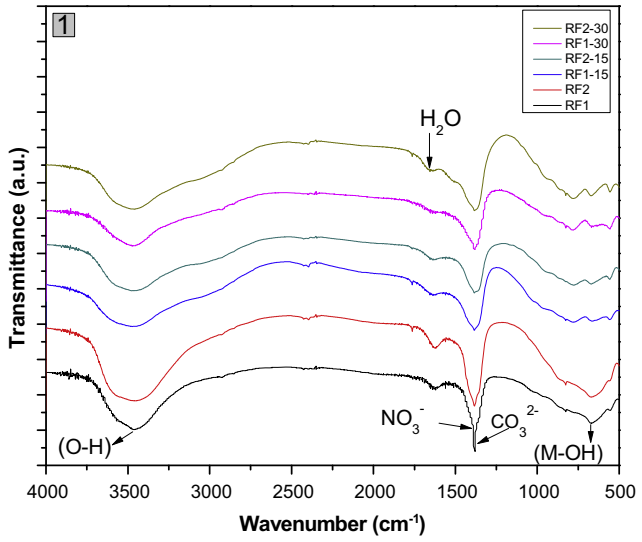

Fig. 2. FT-IR spectra of for fresh KF-loaded MgCaAl LDH.

Fe, Co, Cu, Ni or Zn) and M^{3+} (M = Al, Cr, Ga, Mn or Fe) are di- and trivalent cations, respectively; the value of x is equal to the molar ratio of $M^{2+}/(M^{2+} + M^{3+})$ and; A^{n-} is the anion in compensating charge position with exchangeable capacity [23,24].

Specially, the mixed oxides obtained from LDHs impregnated with KF have shown interesting results in the transesterification of palm oil, such as LDH KF/Mg–Al, which exhibited a FAME yield near of 85% [25]. In the system LDH KF/Ca–Al, 95.6% FAME yields was reached [26], whereas in the LDH KF/Ca–Mg–Al was presented a FAME yield 98% [27]. In these works, the mass ratio of KF was 1:1, with higher methanol/oil molar ratio 12:1. Additionally, it has been reported that this family of materials shows great stability after many reuse cycles in the transesterification reaction [28–30].

Thus, the increasing of global demand for energy and environmental awareness has prompted many researchers to embark on fuel platforms that are environmentally-friendlier alternatives. Biodiesel (a mixture of fatty acid methyl esters, FAMEs) has become very attractive as a biofuel because of its environmental benefits, it has less air pollutants per net energy than diesel, since it decreases the effect of acid rain and is nontoxic and biodegradable; biodiesel sources are renewable and they offer enormous opportunity in bio-based economy market [31].

In this work, a series of LDH MgCaAl modified with KF were synthetized, the effect of divalent cations ratio and KF load were studied in the transesterification reaction of *Jatropha curcas* oil to obtain biodiesel employing inedible oil, low methanol/oil ratio, and short reaction time.

2. Experimental

2.1. LDH MgCaAl materials preparation

Hydrotalcite-like compounds MgCaAl with Al/Mg atomic ratio of 3 and varying the Mg/Ca ratio were prepared by coprecipitation method at pH ≈ 11 of suitable amounts of $Mg(NO_3)_2{\cdot}6H_2O$, $Ca(NO_3)_2{\cdot}4H_2O$, $Al(NO_3)_3{\cdot}6H_2O$ with a 2.0 M solution of NaOH (Aldrich). The addition of the alkaline solution and pH were controlled by pH-STAT Tritando apparatus (Metrohm). The suspension was stirred overnight at 80 °C, and the solid was then separated by centrifugation, rinsed thoroughly with distilled water (Na < 100 ppm), and dried overnight at 80 °C. The LDH were heat-activated in air flow at 450 °C during 4 h (heating rate: 2 °C/min) to yield the $M^{II}(M^{III})O$ mixed oxide. Samples were labeled as HFX where F means fresh, X is Mg/Ca ratio.

2.2. Catalysts preparation by KF impregnation

LDHs MgCaAl were modified by impregnation of KF using the incipient wetness method, the solids were prepared containing 5, 15 and 30 wt% of KF. After the impregnation the solids were dried overnight at 80 °C and heat-activated in air flow at 450 °C for 4 h (heating rate: 2 °C/min). Materials were labeled as RC(F)X-Y, where C or F means calcined or fresh, X is Mg/Ca ratio, and Y indicates KF content.

2.3. Physicochemical characterization

2.3.1. XRD

XRD patterns of the samples as prepared or calcined at 450 °C were recorded on a Philips XPert diffractometer employing Cu K_α radiation (λ = 1.5418 Å) operating at 45 kV and 40 mA in the range of 4–80°.

2.3.2. Textural analysis

The nitrogen adsorption–desorption isotherms, N_2 sorption experiments at 77 K were carried out on samples previously calcined at 450 °C and outgassed at 280 °C for 10 h (10–4 Pa), analysis were determined by Bel-Japan Minisorp II equipment, using a multipoint technique. Surface areas were calculated with the BET equation, and pore diameter values were calculated using the BJH method.

2.3.3. FT-IR and ^{27}Al and ^{19}F MAS NMR spectroscopies

Absorption/transmission IR spectra were run at RT on a Magna-IR Nicolet 750 spectrophotometer, working in the range of wavenumbers 4000–400 cm^{-1} at a resolution of 4 cm^{-1} (number of scans ~ 64).

Solid-state ^{27}Al and ^{19}F Nuclear Magnetic Resonance (MAS NMR) single excitation experiments were performed on a Bruker Avance 300 spectrometer at frequency of 104.2 MHz, and were acquired using the combined techniques of Magic Angle Spinning (MAS) and Proton Dipolar Decoupling (HPDEC). Direct pulsed NMR excitation was used throughout, employing 90° observing pulses (3 μs) with a pulse repetition time of 40 s. Powdered samples were packed in zirconia rotors. The spinning rate was 5 kHz. Chemical shifts were referenced to TMS. ^{27}Al MAS NMR spectra were acquired using short single pulses (π/12) and a delay of 0.5 s. The samples were spun at 10 kHz, and the chemical shifts were referenced to an aqueous 1 M $AlCl_3$ solution.

The ^{19}F MAS NMR spectra were measured by operating the spectrometer at 376.3 MHz, using π/2 pulses of 6 ms with a recycle delay of 1 s. ^{19}F chemical shifts were referenced to those of $CFCl_3$ at 0 ppm.

2.4. Catalytic evaluation in the transesterification reaction

J. curcas oil was provided by local producers from Chiapas, Mexico, it was used as received, and methanol was reagent grade (Aldrich, 99%). The catalytic reaction was carried out in a batch reactor operation at atmospheric pressure under the next conditions: temperature of 60 °C, molar ratio methanol:oil = 6:1, catalyst (calcined) = 3.6 wt%, reaction time = 4 h, the suspension was stirred in refluxing. After the reaction time, the catalyst was separated by filtration; methanol excess was recuperated by distillation and the phase containing biodiesel was isolated from the glycerol formed.

Biodiesel (FAME) identification and quantification was obtained by ^{1}H NMR spectroscopy using a Bruker Avance 300 spectrometer at frequency of 500.13 MHz at 25 °C in a probe with external diameter of 4 mm, the solvent was $CDCl_3$ and TSM as internal standard. Conversion to biodiesel was calculated by integration of signals employing the next equation.

$$X = 100 * \left(\frac{2A_{ME}}{3A_{\alpha-CH_2}}\right)$$

where X = triglycerides conversion to FAME, A_{ME} = integration value of FAME, signal at δ 3.7, and $A_{\alpha-CH_2}$ = integration value of methyl proton, signal at δ 2.3.

Table 1
Textural properties of calcined KF/MgCaAl-LDH.

Catalysts	Surface area ($m^2\ g^{-1}$)	Pore diameter[a] (nm)
RC1	180.0	8.8
RC1-15	21.4	31.9
RC1-30	3.7	56.9
RC2	151.2	17.2
RC2-15	26.3	63.6
RC1-30	8.7	72.3

[a] Calculated by BJH method from the desorption isotherm.

3. Results and discussion

3.1. XRD characterization

Fig. 1a shows the XRD patterns for the as-synthetized LDH. The as-synthetized samples show features typically associated with synthetic LDH [23]. The reflections *003*, *006* and *009* are easily identified and the basal spacing can be determined from the *003* position through the Bragg's law giving values of 8.053 and 8.170 Å for the samples RF1 and RF2, respectively. These results allow to confirm the presence of nitrate anions in the interlamellar space. The *a* parameter ($a = 2d_{110}$) reflects the average cation-cation distance inside the brucite-like sheets, and its tendency helps to analyze, in this case, the isomorphic substitution of Mg^{2+} by the Ca^{2+} cations. These values are 3.0308 and 3.0215 Å for the samples RF1 and RF2, respectively. As the ionic radii for Ca^{2+} is bigger than that one for Mg^{2+}, the sample RF1 which have more calcium ($Mg^{2+}/Ca^{2+} = 1$) shows a higher *a* value than the sample RF2 ($Mg^{2+}/Ca^{2+} = 2$), indicating that a part of Mg^{2+} cations were replaced by bigger Ca^{2+} cations. Additionally, the sample RF1 shows additional signals located at 18.59°, 19.06° and 40.71° indicating the presence of a segregated phase, which could not be identified. This phase could be related to Ca-compounds.

Upon incorporation of KF over the as-synthetized LDH, the XRD patterns become complex and, besides some signals of LDH still visible, new signals appeared (Fig. 1b and c). In all samples, these new signals cannot be attributed to KF but to other crystalline phases indicating that the initial LDH might have reacted with KF. All the new crystalline phases identified are fluorides derivatives, mainly $KMgF_3$ (JCPDS 01-086-2480), $KCaF_3$ (JCPDS 03-0567), $CaAlF_5$ (JCPDS 03-1060), $KCaCO_3F$ (JCPDS 44-085), and $CaCO_3$ (JCPDS 05-0586). This results agreed those previously reported by Gao et al. [27] whose results indicated that KF/Mg–Al HT showed peaks attributed to $KMgF_3$; KF/Ca–Al HT exhibited peaks belonging to $KCaF_3$, $CaAlF_5$ and $KCaCO_3F$, and finally KF/Ca–Mg–Al HT presented a combination of the above mentioned four phases.

Fig. 1d, corresponds to the calcined samples at 450 °C, coming from the samples of Fig. 2 (RF1-30 and RF1-15), both with a Mg/Ca molar ratio of 1, while Fig. 1e is for calcined samples with a Mg/Ca molar ratio of 2, coming from the samples of Fig. 1c (RF2-30 and RF2-15). The XRD powder diffraction patterns of the samples in Fig. 1d and e (RCX-Y), as expected, show reflections that can be assigned to MgO periclase phase together with those previously observed over the fresh samples, $KMgF_3$, $KCaF_3$, $CaAlF_5$, and $KCaCO_3F$ that were preserved. In addition to the mentioned phases, some CaO was also detected as observed in other works [18]. The signals belonging to the phases that contain calcium became more intense as the calcium loading rises.

3.2. FT-IR analysis

Fig. 2 shows the FT-IR spectrum in the region between 500 and 4000 cm^{-1} for both pristine MgCaAl LDH and for the freshly KF loaded materials. Regarding its composition the IR-active vibrations of layered double hydroxides can be grouped into three categories: molecular vibrations of the hydroxyl groups, lattice vibrations of the octahedral layers and vibrations of the interlayer species. Although, all samples show rather similar spectra, subtle differences can be noted. All spectra show a very intense broad band at approximately 3450 cm^{-1} corresponding to the stretching mode of hydroxyl groups in the brucite-like sheets. This band also involves the stretching mode of interlayer water molecules, as well as the modes corresponding to the layer hydroxyl groups. The weak band at 1640 cm^{-1} is attributed to the deformation mode

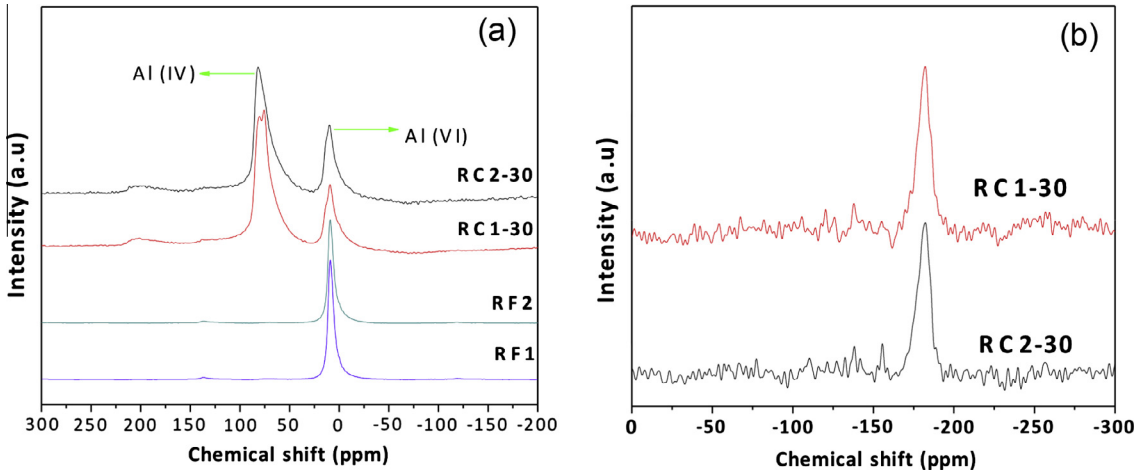

Fig. 3. (a) ^{27}Al RMN MAS spectra of samples: RF1, RF2, RC1-30, RC2-30. (b) ^{19}F RMN MAS spectra of impregnated and calcined LDH materials.

of interlayer water molecules. The strong band at 1380 cm^{-1} is assigned to mode ν_3 of interlayer NO_3^- species. This band becomes broader as the presence of co-intercalated CO_3^{2-} increases due to CO_2 contamination during synthesis. In fact, a band at 1360–1370 cm^{-1} is always associated with the interlayer carbonate. The region comprised between 1200 and 500 cm^{-1} gives information about lattice vibrations. The rather complex group of bands observed at 500–1000 cm^{-1} is manly assigned to hydroxyl M-OH translation modes and the specific position depends on the nature of the M^{2+} or M^{3+} ions [32]. None appreciable modification by the presence of deposited KF over the FTIR spectra of LDH was observed.

3.3. Nitrogen physisorption

The N_2 adsorption isotherms for calcined MgCaAl and KF/MgCaAl LDHs for both parent mixed oxides RC1-Y and RC2-Y showed a very well defined type IV, according to the classification of IUPAC, characteristic of mesoporous solids. This mesoporous character is gradually lost after KF is loaded and finally the isotherm becomes type III for high KF loadings. Surface areas of the supports and catalysts are listed in Table 1. As shown in Table 1, the MgCaAl(O) mixed oxides RC1-Y and RC2-Y shows lower specific surface areas than calcined MgAl LDH that can reach specific surface areas as high as 280 m^2/g [33]. This decrease in specific surface areas can be attributed to the calcium incorporation. In fact, CaAl(O) mixed oxides derived from CaAl LDH show very low surface area (less than 50 $m^2\ g^{-1}$) [34]. Besides, all KF loaded catalysts presented lower surface areas compared to the supports. This drop in BET specific surface area, increased with the KF loading amount, indicates that the deposited material blocks the entrance of the pores. Regarding the pore diameters, it can be observed that as KF loading increases, the pore diameter becomes higher, indicating that the surface might be chemically modified and new species could be created. This statement is also supported by the XRD results.

3.4. Multinuclear ^{27}Al and ^{19}F MAS NMR

Fig. 3a displays ^{27}Al MAS NMR spectra of fresh samples (RF1 and RF2) where only a narrow isotropic peak close to 7 ppm is observed, supporting that aluminum is 6-fold coordinated to oxygen atoms in an octahedral environment. Thus, the aluminum in both samples is part of the brucite-like layers. In contrast, the spectra of thermal treated samples present clearly two signals assigned to Al 6-fold coordinated (peak at 5.3 ppm) and Al 4-fold coordinated (peak at 75 ppm), which is in agreement with the transformation from layered hydrotalcite towards mixed oxide Mg(Al)O with a periclase-like structure [35,36]. Note that the NMR peaks of the thermal treated samples are broader than those of fresh samples which is usually found because of the absence of hydration water molecules that homogenize the electronic environment of aluminum atoms. Actually, the peak corresponding to tetrahedral aluminum in spectrum of RC1-30 is finer than in RC2-30. In spectrum of RC1-30 two tetrahedrical environments seem to be resolved which is probably due to the higher content of calcium, i.e. that the second neighbors of tetrahedral aluminum differs in the number of calcium atoms.

^{19}F MAS NMR spectra of calcined samples, Fig. 3b, shows that fluorine is stabilized on both samples RC1-30 and RC2-30. Regardless of the Mg/Ca ratio only a single peak is observed at −182 ppm. The assignation of this peak is not evident. The chemical shift of KF appears at −140 ppm discarding that KF remains after calcination. On the other hand, CaF does not form because the signal of these species is expected at weaker field. Previously, it was reported the ^{19}F NMR signal for AlF_6 appears at −190 ppm, but that of AlO_5F was reported to be at −120 ppm [37–39]. Thus, it can be assumed that during thermal treatment the fluorine is attached to surface of mixed oxide to give chemical species such as $AlF_{6-x}O_x$. Now, coming back to chemical shift at −182 ppm, it is closer to −190 ppm and it should be concluded that enriched fluorine $AlF_{6-x}O_x$ species are formed. The fluorination of mixed oxide Mg(Al)O emerged from the thermal treatment of LDH was reported, but a better distribution of fluorine was obtained because of the method used by Lima et al. [40]. In our case, the impregnation seems to be more local avoiding a high dispersion of fluorine into the structure of mixed oxide. Besides, from NMR results it is well known that mixed oxides can be rehydrated-calcined without any significant structural changes.

3.5. Transesterification reaction

Fig. 4a shows the ^{1}H NMR spectrum of *J. curcas* oil, characteristic signals appear between 4.1 and 4.3 ppm generated by the CH_2-O protons from the triglycerides. The signals around 5.4 ppm are associated to the total olefinic protons of unsaturated fatty acids. From this, typical composition of oleic and linoleic as principal fatty acid was observed.

Preliminary catalytic reactions were carried out with as prepared materials after KF impregnation (non calcined), the results showed any catalytic activity for all samples.

As mention in the experimental section, ^{1}H NMR technique was employed for biodiesel quantification using calcined materials. In

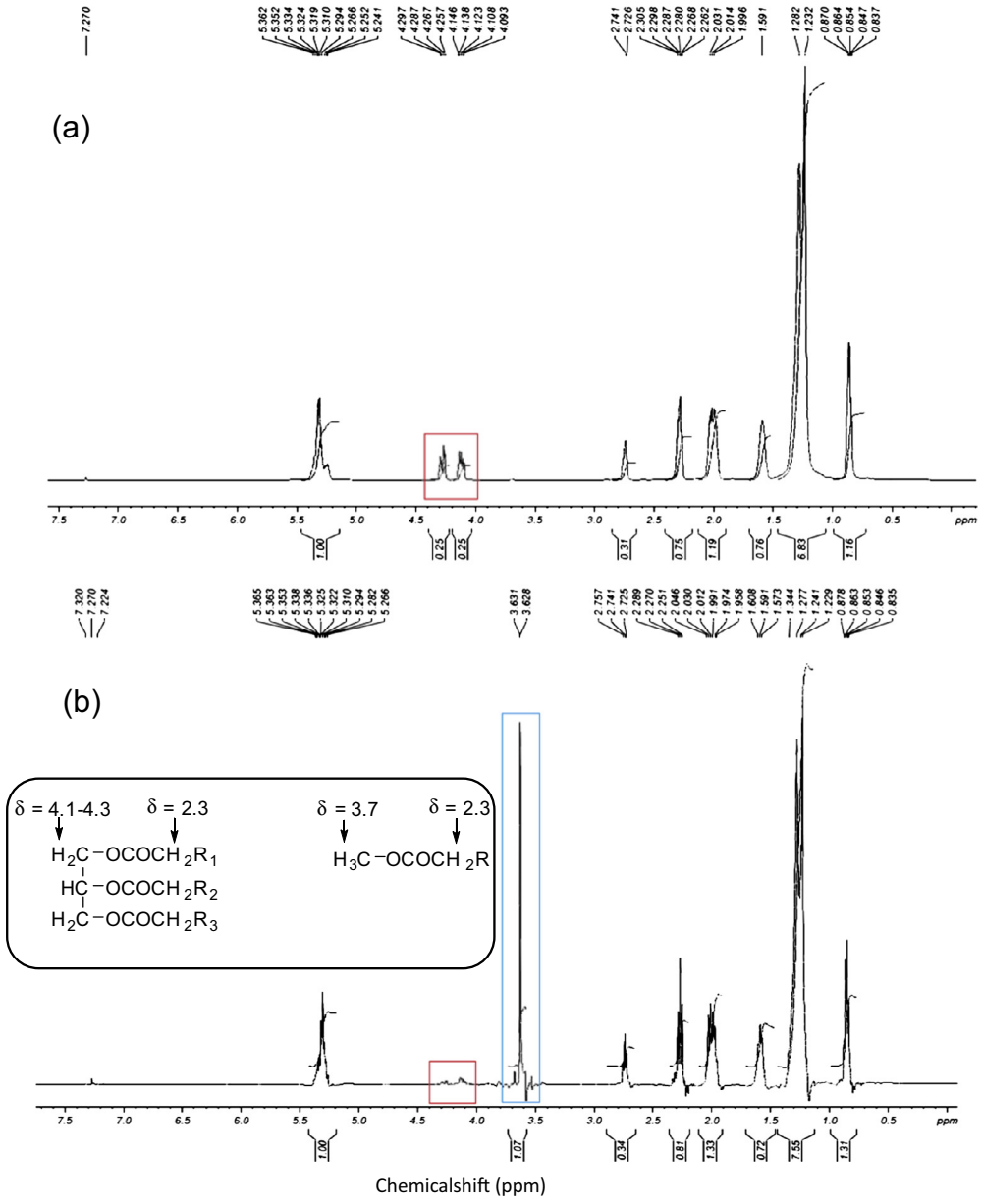

Fig. 4. ^{1}H NMR spectrum (a) *Jatropha curcas* oil and (b) biodiesel product (FAME) of transesterification of *Jatropha curcas* oil with KF MgCaAl catalysts. Inset: ^{1}H NMR signals used for identification and quantification of FAME formation.

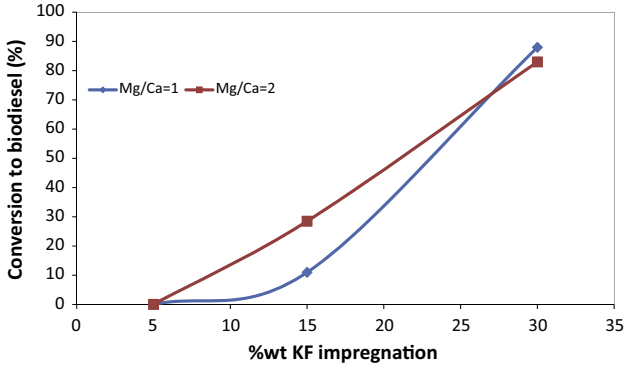

Fig. 5. Influence of KF/MgCaAl catalysts composition in biodiesel production.

Fig. 4b the spectrum recorded after reaction is showed. It can be observed the evolution on two regions, the decrease of signals between 4.0 and 4.5 ppm and the apparition of singlet band around 3.7 ppm, and this last is attributed to methoxy group associated to biodiesel formation (FAME). The triplet at 2.3 ppm, is related to α-CH_2 protons to the esther carbonyl, of both FAME and the starting *J. curcas* oil (see insert in Fig. 4b).

Fig. 5 correlates conversion to biodiesel and KF content for catalysts with different Mg/Ca ratio. Comparing at low conversion, the effect of Mg/Ca ratio with the same KF content, it is clear the influence of Ca, the RC1-15 (Mg/Ca = 1) achieved around 10% conversion while for the catalyst RC2-15 (Mg/Ca = 2) reached 28%. Nevertheless, the effect of KF was more notorious in both materials at higher conversions. In this case, around 90% conversion was reached at higher KF contents.

It should be notice from preliminary catalytic tests, carried out using non calcined samples, that the nature of the basic sites present in the materials plays a central role on the performance of the transesterification reaction. Since it was not catalytic activity for the as prepared materials, it can be concluded that this reaction is highly sensitive to the basicity of lattice oxygen atoms

(Lewis sites), obtained after thermal treatment of the samples, and not from the hydroxyls groups (Brønsted sites) present in the as prepared materials [41,42].

On the other hand, the performance of catalytic activity can be moreover associated to base properties generated by the mixed oxides and the presence of stable fluorinated species. According to Gao et al. [27], Ca^{2+} has an important influence on the LDH layers structure and the fluorinated species formed, which act as active catalytic centers. Moreover, it was reported by Wang et al. [17] that the presence of KF, Mg and Ca oxides increase the resistance to acid attack. In our materials, both oxides are formed after thermal treatment as part of the mixed oxides when LDH structure collapses. Additionally, the catalysis performance is associated to different fluorinated species formed, playing an important role, these species were detected by DRX and ^{19}F RMN showing good stability. It has been already reported that K could leach from the solid catalyst into the liquid phase [43], however, in our case the amount of potassium is not as high because of the stabilization of the fluorine-oxygen-aluminum species. Then, it is assumed that catalysis occurs through these species easily regenerated by the memory effect of the hydrotalcite-like compounds.

4. Conclusions

XRD analysis showed typical diffraction patterns of hydrotalcite-like compounds, while for the impregnated samples after calcination the profiles exhibited the mixed oxide formed. In addition, other peaks appeared and they were associated to the formation of fluorinated species. By nitrogen physisorption, the mixed oxides mesoporous materials were also confirmed. ^{27}Al NMR spectra showed bands at 10 and 88 ppm attributed to the Al coordination. For impregnated samples with KF, a main signal at −180 ppm was observed, indicating the presence of tetrahedral aluminum fluorinated species of LDH as detected by XRD.

The results of the transesterification reaction showed a meaningfully correlation between the nature of the basic sites (fluorinated species), the Mg/Ca ratio, and the KF content in the oil conversion to biodiesel. The higher conversion was achieved c.a. 90% when Mg/Ca = 1 and KF load was 30 wt%. It should be mentioned that the methanol: oil ratio and KF load were lower comparing with others studies. These results showed that the good balance of the physicochemical properties of the catalytic materials can achieve high values of conversion for the biodiesel production.

Acknowledgments

Projects SIP-IPN 20140793, CONACYT Projects 101319, INFRA2014 225161.

References

[1] M.D. Serio, R. Tesser, L. Pengmei, E. Santacesaria, Energy Fuels 22 (2008) 207.
[2] S.L. Martínez, R. Romero, J.C. Lopez, A. Romero, V.S. Mendieta, R. Natividad, Ind. Eng. Chem. Res. 50 (2011) 2665.
[3] W. Charusiri, Energy Fuels 19 (2005) 1783.
[4] X. Hu, Z. Zhou, D. Sun, Y. Wang, Z. Zhang, Catal. Lett. 133 (2009) 90.
[5] C. Witchakorn, V. Tharapong, Energy Fuels 19 (2005) 1783.
[6] J.A. Anderson, A. Beaton, A. Galadima, R.P.K. Well, Catal. Lett. 131 (2009) 213.
[7] Y. Liu, R. Sotelo-Boyás, K. Murata, T. Minowa, K. Sakanishi, Chem. Lett. 38 (2009) 552.
[8] I. Lukic, J. Krstic, D. Jovanovic, D. Skala, Biores. Technol. 100 (2009) 4690.
[9] J. Ni, D. Rooney, F.C. Meunier, Appl. Catal. B 97 (2010) 269.
[10] M. Verziu, M. Florea, S. Simon, V. Simon, P. Filip, V.I. Parvulescu, C. Hardacre, J. Catal. 263 (2009) 56.
[11] J.F.P. Gomes, J.F.B. Puna, L.M. Gonçalves, J.C.M. Bordado, Energy 36 (2011) 6770.
[12] M.L. Granados, D.M. Alonso, A.C. Alba-Rubio, R. Mariscal, M. Ojeda, P. Brettes, Energy Fuels 23 (2009) 2259.
[13] Z. Helwani, N. Aziz, M.Z.A. Bakar, H. Mukhtar, J. Kim, M.R. Othman, Energy Convers. Manage. 73 (2013) 128.
[14] E. Li, Z.P. Xu, V. Rudolph, Appl. Catal. B 88 (2009) 42.
[15] H. Liu, L. Su, Y. Shao, L. Zou, Fuel 97 (2012) 651.
[16] I. Reyero, I. Velasco, O. Sanz, M. Montes, G. Arzamendi, L.M. Gandía, Catal. Today 216 (2013) 211.
[17] Y. Wang, S. Hu, Y. Guan, L. Wen, H. Han, Catal. Lett. 131 (2009) 574.
[18] L. Wen, Y. Wang, D. Lu, S. Hu, H. Han, Fuel 89 (2010) 2267.
[19] C. Xu, D.I. Enache, R. Lloyd, D.W. Knight, J.K. Bartley, G.J. Hutchings, Catal. Lett. 138 (2010) 1.
[20] S. Furuta, H. Matsuhashi, K. Arata, Catal. Commun. 5 (2004) 721.
[21] K. Narasimharao, D.R. Brown, A.F. Lee, A.D. Newman, P.F. Siril, S.J. Tavener, K. Wilson, J. Catal. 248 (248) (2007) 226.
[22] A. Zieba, L. Matachowski, E. Lalik, A. Drelinkiewicz, Catal. Lett. 127 (2009) 183.
[23] F. Cavani, F. Trifiro, A. Vaccari, Catal. Today 11 (1991) 173.
[24] S. Miyata, Clays Clay Miner. 28 (1980) 50.
[25] L. Gao, B. Xu, G. Xiao, J. Lv, Energy Fuels 22 (2008) 3531.
[26] L. Gao, G. Teng, G. Xiao, R. Wei, Biomass Bioenergy 34 (2010) 1283.
[27] L. Gao, G. Teng, J. Lv, G. Xiao, Energy Fuels 24 (2010) 646.
[28] C.S. Castro, L.C.F. Garcia Júnior, J.M. Assaf, Fuel Process. Technol. 125 (2014) 73.
[29] J. Chen, L. Jia, X. Guo, L. Xiang, S. Lou, RSC Adv. 4 (2014) 60025.
[30] P. Kutáleka, Libor Čapeka, L. Smoláková, D. Kubička, Fuel Proc. Technol. 122 (2014) 176.
[31] G. Knothe, C.A. Sharp, T.W. Ryan, Energy Fuels 20 (2006) 403.
[32] J.T. Kloprogge, R.L. Frost, J. Solid State Chem. 146 (1999) 506.
[33] J. Shen, J.M. Kobe, Y. Chen, J.A. Dumesic, Langmuir 10 (1994) 3902.
[34] E. López-Salinas, M.E. Llanos-Serrano, M.A. Cortés-Jácome, I. Schifter-Secora, J. Porous Mater. 2 (1996) 291.
[35] M.C.I. Bezen, C. Breitkopf, J.A. Lercher, ACS Catal. 1 (2011) 1384.
[36] J.S. Valente, E. Lima, J.A. Toledo-Antonio, M.A. Cortes-Jacome, L. Lartundo-Rojas, R. Montiel, J. Prince, J. Phys. Chem. C 114 (2010) 2089.
[37] P.J. Chupas, C.P. Grey, J. Catal. 224 (2004) 69.
[38] H.A. Prescott, Z.-J. Li, E. Kemnitz, J. Deutsch, H.J. Lieske, J. Mater. Chem. 15 (2005) 4616.
[39] G. Scholz, C. Stosiek, J. Noack, E. Kemnitz, J. Fluorine Chem. 132 (2011) 1079.
[40] E. Lima, M.J. Martínez-Ortiz, R.I. Gutiérrez-Reyes, M. Vera, Inorg. Chem. 51 (2012) 7774.
[41] F. Prinetto, G. Ghiotti, R. Durand, D. Tichit, J. Phys. Chem. B 104 (2000) 11117.
[42] J.S. Valente, F. Figueras, M. Gravelle, P. Kumbhar, J. Lopez, J.P. Besse, J. Catal. 189 (2000) 370.
[43] L. Čapek, M. Hájek, P. Kutálek, L. Smoláková, Fuel 115 (2014) 443.